Size-dependent blinking of molecular aggregate total emission

V V Savchenko[1,2], **A A Zimin**[1,2], **N Yu Ignatova**[1,2], **V Kimberg**[1,2], **F Gel'mukhanov**[1,2], **S P Polyutov**[1]

[1]Institute of Nanotechnology, Spectroscopy and Quantum Chemistry, Siberian Federal University, Krasnoyarsk, 660041, Russia
[2]Department of Theoretical Chemistry and Biology, KTH Royal Institute of Technology, Stockholm, Sweden

E-mail: `vvsavchenko@sfu-kras.ru`

Abstract. Molecular aggregates are well known for their customizable optical properties. Vibronic coupling in monomers forming such aggregates offers rich opportunities for property tuning. We study generic molecular aggregate models of growing complexity (from a dimer up to a decamer) and report how vibronic coupling affects aggregate fluorescence intensity. The total aggregate fluorescence intensity is a measure sensitive to both vibronic coupling and Coulomb coupling between monomer transition densities. Using an exact diagonalization approach in the two-particle basis set, we show how the interplay between Coulomb and vibronic coupling affects aggregate fluorescence. Moreover, for H-aggregates we predict a periodic variation of the fluorescence intensity with aggregate size and show that vibronic interaction decreases the effect.

1. Introduction

The investigation of molecular aggregates (MAs) opens the possibility of creating new promising materials for optical technologies [1, 2, 3]. Photophysical properties of vibronic excitation in MAs are of crucial importance for systems ranging from organic dye solutions to artificial photosynthetic devices. One of widely used methods to employ exciton-vibrational coupling in dynamics and spectroscopy of MAs is to use the theory of open systems by putting low-frequency vibrational degrees of freedom in a thermal reservoir characterized by its spectral function [2], whereas only the important degrees of freedom (typically only electronic) are included in a system Hamiltonian. However, recent research [4, 5, 6, 1, 7] show that this way is not always appropriate for calculations of optical response and study of exciton dynamics of such aggregates. These recent contributions have spurred interest to the exciton-vibrational coupling problem in molecular aggregates and resulted in a revision of theories of energy transfer and coherence in MAs, in particular, by explicit inclusion of a quantized vibrational mode in the system Hamiltonian.

In recent years methods of direct diagonalization of Hamiltonian with respect to the vibronic problem have attracted much attention [1, 8, 5, 9, 10, 11, 7, 6] especially in the context of the role of vibronic coherence in the light-harvesting machinery [12, 13, 14, 15, 4]. Another application of this method is a modelling of MAs structure with specified properties and revealing of MAs structure and the dynamics of aggregation [16]. One of the most interesting of MAs is a perylene

bisimide (PBI) aggregate. An experiment with this dye shows unusual temperature-dependent emission spectra behaviour and motivates to study this aggregate in details [17, 16]. Here we study the fluorescence intensity of vibronic H-aggregates on a generic model of growing complexity using the exact diagonalization approach in the two-particle basis set [18].

2. Theory

The Hamiltonian of the molecular aggregate is represented as:

$$H = \sum_A |g^A\rangle H_g^A \langle g^A| + |e^A\rangle H_e^A \langle e^A| + \sum_{A>B} \left(|g^A e^B\rangle J^{AB} \langle e^A g^B| + c.c. \right),\tag{1}$$

where $|g^A\rangle$ and $|e^A\rangle$ are electronic eigenstates for monomer A in ground and excited states, respectively, indices A and B run over all monomers in the aggregate, H^A is the appropriate Hamiltonian for isolated monomer A, J^{AB} represents the Coulomb coupling term between electronic transition densities on monomers A and B, c.c. stands for complex conjugate terms (see [1] for theoretical details). Strength of the vibronic coupling is quantified by the Huang-Rhys parameter S. The population of energy states is described by Bose-Einstein distribution $N_{BE} = (exp[(E - E_F)/k_B T] - 1)^{-1}$, where k_B=3.16681 Eh/K with temperature T, E is state energy, E_F is the chemical potential (Fermi level). Monomer ground and excited potential energy surfaces (PES) are taken to be harmonic, with excited state minimum being displacement by $(2S)^{1/2}$ relative to the ground state. Emission intensity is computed as: $F(\omega) = \Sigma_{i,f} |\langle f|d_{el}|i\rangle|^2 \delta(\omega - \omega_{if})$, where the summation goes over all initial and final states, d_{el} is the electronic transition tor, and ω_{if} is the transition energy. Integrated emission is then obtained as $I_{ems} = \Sigma_\omega F(\omega)$. Note that we simplify our definition of emission by dropping out all factors excepts for transition amplitude.

The aggregate Hamiltonian is then expressed in the two-particle basis set of the form (here shown for tetramer) $|e^A, \nu^A\rangle \otimes |g^B, \nu^B\rangle \otimes |g^C, 0\rangle \otimes |g^D, 0\rangle$, where capital letters are used to index monomers and ν denotes a variable number of vibrational quanta in a particular mode for ground (g) or excited (e) PES. Only single-exciton manifold is required for our purposes. "Two-particle" means that no more than two vibrationally excited monomers enter the basis function at the same time, one of them being in electronically excited state. Physically, two-particle basis set is required to take excitonic polaron formation into account, resulting from deformation (vibrational excitation) of monomers surrounding a vibronically excited monomer. Strictly speaking, a general N-particle basis is required for an aggregate of size N, quickly making exact diagonalization approach unfeasible for $N > 3$. Two-particle basis set is sufficient for description of low-energy aggregate eigenstates when Coulomb coupling is comparable to vibrational mode energy ω_{vib}. Details of our theoretical approach can be found in [1]. Our methodology is formulated in the eigenstate representation and is not limited to the case of harmonic potential energy surfaces – vibronic coupling is hidden in the Franck-Condon overlap integrals. In particular, application to energy transfer problems with explicit inclusion of a quantized vibrational mode in condensed systems such as liquid water solutions or doped semiconductors are possible, given the availability of the monomer potentials.

3. Results and discussion

We begin by comparing energy levels of excitons in purely electronic aggregates with vibronic aggregates, limiting ourselves to dimer, trimer and tetramer (Figure 1 (a), (b) and (c), respectively). Aggregates are modeled as a linear chain of monomers with their transition dipole moments aligned either in a head-to-tail fashion (J-aggregates and negative Coulomb coupling), or in a parallel arrangement orthogonal to the aggregate axis (sandwiched H-aggregates). Excitonic states are labeled $|\alpha_1\rangle$ through $|\alpha_4\rangle$. Square of the transition dipole

moment ($d_i = \langle 0|\mathbf{d}_{el}|\alpha_i\rangle$) from each of these states to the (vibrationless) ground state is shown in the figures in the middle, whereas excitonic energy levels for the corresponding vibronic aggregates are located at the bottom. Here E is the eigenstate energy, E_{00} is the electronic vertical transition energy. Vibrational mode frequency is 1500 cm^{-1}.

Electronic dimer behaves symmetrically with respect to the sign change of Coulomb coupling (Figure 1(a)). Transitions to the ground state form either $|\alpha_1\rangle$ or $|\alpha_2\rangle$ are allowed for J-dimer and H-dimer, respectively. Energy levels are separated by twice the Coulomb interaction strength $2J$. Situation becomes more complicated when the vibronic coupling is included. When there is no Coulomb coupling between monomers, we obtain a set of degenerate monomer vibronic energy levels located at integer multiples of vibrational mode frequency. These "bands" lose degeneracy as Coulomb coupling strength is increased.

Energy levels for electronic trimer, as well as transition dipole moments to the ground state and vibronic trimer energy levels are shown in Figure 1(b). Note the antisymmetry of $|\alpha_2\rangle$ excitonic state energy with respect to change of Coulomb coupling sign, whose energy behaves analytically as $E_{00}-J_{13}$, where J_{13} is the strength of Coulomb coupling between edge monomers. This example illustrates that by taking only nearest-neighbor Coulomb coupling into account for vibronic trimer we get an error in eigenstate energies on the order of J_{13}. In contrast to H-dimer, H-trimer does not have full compensation of the transition amplitude form the lowest-energy eigenstate $|\alpha_1\rangle$. This antisymmetry further manifests itself in the energies of excitonic states for vibronic trimer on the bottom of the Figure 1(b). Electronic and vibronic tetramers follow the same tendency, as shown in Figure 1(c).

The total absorption intensity is independent of the temperature and interaction strength in accordance with the total dipole moment square conservation law in the described systems, but this is not the case for emission. The vibrational energy redistribution of exciton states in accordance with the temperature can lead to the fact that a significant transition portion from populated states to the ground vibronic global state can be forbidden by dipole moment. Thus, the total emission intensity is not retained. In Figures 2 (a, b) and 3 (a,b) we can observe features that forbidden transitions in H-aggregate become allowed due to odd number of monomers in molecular aggregates. The odd number of monomers line up in a molecular aggregate so that it leads to intermediate molecular configuration. This effect appear not in all cases.

Next, we study the integrated aggregate fluorescence intensity as a function of three parameters: number of monomers (N), vibronic coupling strength (S) and Coulomb coupling strength between monomers (J). Figure 2 shows a (S,N) plane for two Coulomb couplings $J = \omega_{vib}/3$ and $J = \omega_{vib}$, whereas (J,N) plane is shown in Figure 3 for two Huang-Rhys factors $S = 0.05$ and $S = 0.4$. Units are chosen relative to the monomer integrated fluorescence intensity.

The role of Coulomb coupling for vibronic H-aggregates is twofold: weak coupling ($\omega_{vib}/3$, Figure 2(a)) regime allows to gain about 20-30% of monomer fluorescence intensity for all N, given sufficiently large vibronic coupling strength. Increasing aggregate size requires increase in S to obtain such gains. However, when Coulomb coupling strength is increased, we see a rapid drop to only about 14% of monomer intensity at best for dimer at $S = 1$. Aggregates of larger size show heavily quenched fluorescence (Figure 2(b)). Overall, increasing vibronic coupling strength opens additonal emission channels and lifts electronic selection rules.

Fluorescence intensity in the (J,N) plane for two Huang-Rhys factors, $S = 0.05$ and $S = 0.4$, clearly shows the drastic role of vibronic coupling. For $S = 0.05$ vibronic aggregates behave very similar to the electronic aggregates, as one indeed might expect. Note the oscillatory behavior of the fluorescence intensity with the aggregate parity. On the contrary, up to about 15% of monomer fluorescence intensity can be regained when $S = 0.4$.

Let us note that a dimer has forbidden lowest exciton state (Figure 1), while for a trimer lowest exciton state is allowed and, consequently, a dimer has smaller emission intensity than a trimer.
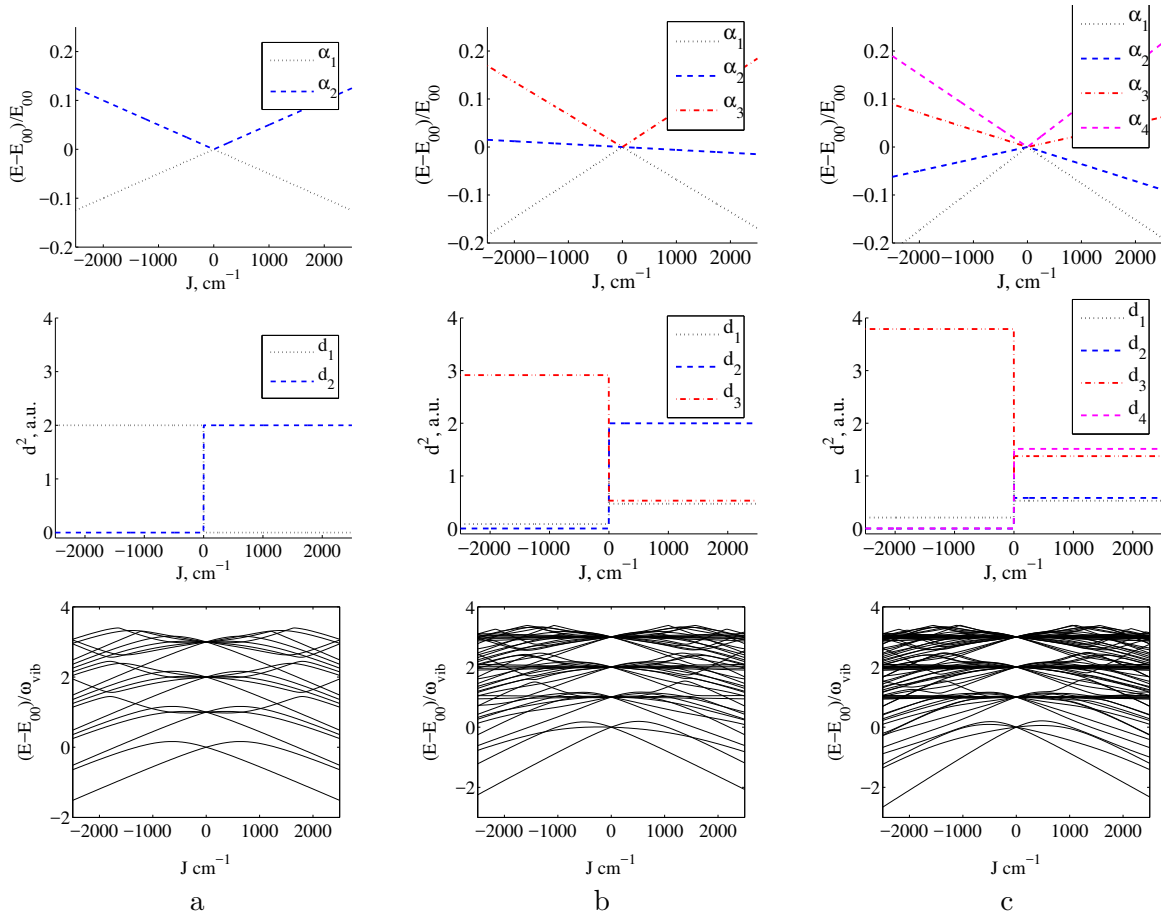
Figure 1. Energy levels of dimer (a), trimer (b) and tetramer (c) for the electronic model (upper panel) and vibronic model (lower panel), respectively. For vibronic case S=0.4. The squared transition dipole moments to the vibrationless aggregate ground state are presented on the middle panel.

The decrease in total emission intensity with increasing J for all aggregate sizes appears due to several factors. First, exciton-vibrational coupling results (a) in exciton states splitting and (b) in transition dipole moments redistribution making some of transitions forbidden. Second, the splitting between exciton states results in different thermalization of exciton states dependent on the coupling. The competition of these factors finally results in observed behaviour.

It is important to note that role of finite-size effects becomes apparent from Figures 2 and 3. For smaller aggregates (up to 5 monomers) fluorescence intensity changes drastically both in (S,N) and in (J,N) planes as number of monomers is increased. As one might expect, for larger aggregates finite-size effects become less pronounced.

Finally, we point out that interplay between Coulomb and vibronic coupling in molecular aggregates is not so straightforward to unravel. Vibronic coupling could enhance aggregate fluorescence intensity for a right choice of parameters – relatively weak Coulomb coupling and strong vibronic coupling. Finite-size effects as well as Coulomb coupling between non-nearest neighbors are important for understanding of the underlying photophysical aspects of molecular aggregates. Detailed studies and simplified theoretical models are required to further explore possibilities for rational design of molecular aggregates with required optical properties.
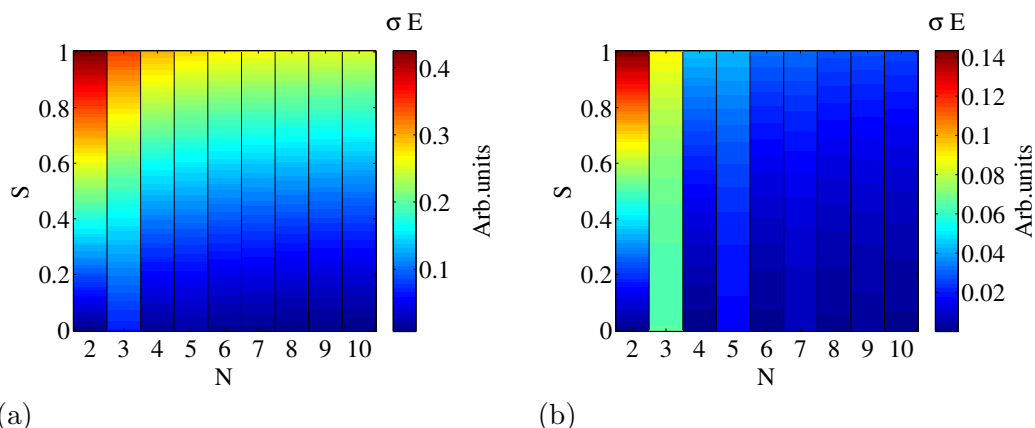
Figure 2. Total emission for J=500 cm^{-1} (panel (a)) and J=1500 cm^{-1} (panel (b)) for different number of monomers N.
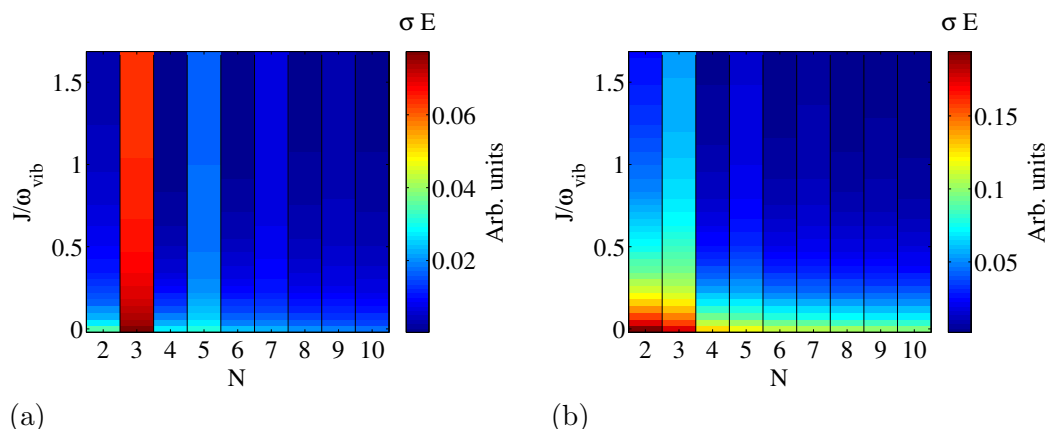

Figure 3. Total emission for Huag-Rhys factors S=0.05 (panel (a)) and S=0.4 (panel (b)) for different number of monomers N.

4. Acknowledgments

References

[1] Schröter M, Ivanov S, Schulze J, Polyutov S, Yan Y, Pullerits T and Kühn O 2015 *Physics Reports* **567** 1–78
[2] May V and Kühn O 2008 *Charge and energy transfer dynamics in molecular systems* (John Wiley & Sons)
[3] Scholes G D, Fleming G R, Chen L X, Aspuru-Guzik A, Buchleitner A, Coker D F, Engel G S, van Grondelle R, Ishizaki A, Jonas D M *et al.* 2017 *Nature* **543** 647–656
[4] Tiwari V, Peters W K and Jonas D M 2013 *Proceedings of the National Academy of Sciences* **110** 1203–1208
[5] Womick J M and Moran A M 2011 *The Journal of Physical Chemistry B* **115** 1347–1356
[6] Polyutov S, Kühn O and Pullerits T 2012 *Chemical Physics* **394** 21–28
[7] Bašinskaitė E, Butkus V, Abramavicius D and Valkunas L 2014 *Photosynthesis research* **121** 95–106
[8] Yang M 2005 *The Journal of chemical physics* **123** 124705
[9] Guthmuller J, Zutterman F and Champagne B 2009 *The Journal of chemical physics* **131** 154302
[10] Guthmuller J, Zutterman F and Champagne B 2008 *Journal of chemical theory and computation* **4** 2094–2100
[11] Myers Kelley A 2003 *The Journal of chemical physics* **119** 3320–3331
[12] Kobayashi T 1996 *J-aggregates* vol 1 (University of Tokyo, Japan: World Scientific)

[13] Spano F C and Mukamel S 1991 *Physical review letters* **66** 1197

[14] Burghardt I, May V, Micha D A and Bittner E R 2009 *Energy Transfer Dynamics in Biomaterial Systems* (Springer)

[15] Christensson N, Kauffmann H F, Pullerits T and Mancal T 2012 *The Journal of Physical Chemistry Part B* **116** 7449–7454

[16] Plötz P A, Polyutov S, Ivanov S, Fennel F, Wolter S, Niehaus T, Xie Z, Lochbrunner S, Würthner F and Kühn O 2016 *Physical Chemistry Chemical Physics* **18** 25110–25119

[17] Fennel F, Wolter S, Xie Z, Plötz P A, Kühn O, Würthner F and Lochbrunner S 2013 *Journal of the American Chemical Society* **135** 18722–18725

[18] Philpott M R 1971 *The Journal of Chemical Physics* **55** 2039–2054